

# Learning Kernels for Structured Prediction using Polynomial Kernel Transformations

Chetan Tonde, Ahmed Elgammal  
 Department of Computer Science, Rutgers University,  
 Piscataway, NJ - 08854 USA.  
 {cjtonde, elgammal}@cs.rutgers.edu

February 12, 2022

## Abstract

Learning the kernel functions used in kernel methods has been a vastly explored area in machine learning. It is now widely accepted that to obtain 'good' performance, learning a kernel function is the key challenge. In this work we focus on learning kernel representations for structured regression. We propose use of polynomials expansion of kernels, referred to as Schoenberg transforms and Gegenbaur transforms, which arise from the seminal result of Schoenberg [1938]. These kernels can be thought of as polynomial combination of input features in a high dimensional reproducing kernel Hilbert space (RKHS). We learn kernels over input and output for structured data, such that, dependency between kernel features is maximized. We use Hilbert-Schmidt Independence Criterion (HSIC) to measure this. We also give an efficient, matrix decomposition-based algorithm to learn these kernel transformations, and demonstrate state-of-the-art results on several real-world datasets.

## 1 Introduction

The goal in supervised structured prediction is to learn a prediction function  $f: \mathcal{X} \rightarrow \mathcal{Y}$  from an input domain  $\mathcal{X}$ , to an output domain  $\mathcal{Y}$ . As an example, in articulated human pose estimation, input  $x \in \mathcal{X}$  would be an image of a human performing an action, and output would be the an interdependent vector of joint positions  $(x, y, z)$ . Typically, space of functions  $\mathcal{H}$  is fixed (decision trees, neural networks, SVMs) and parametrized. We estimate these parameters from a given set of training examples  $S = \{(x_1, y_1), (x_2, y_2), \dots, (x_m, y_m)\} \subseteq \mathcal{X} \times \mathcal{Y}$ , drawn independently identically distributed (i.i.d.) from  $P(x, y)$  over  $\mathcal{X} \times \mathcal{Y}$ . We formulate a meaningful loss function  $\mathcal{L}: \mathcal{Y} \times \mathcal{Y}$ , such as 0-1 loss, or squared loss [Weston et al., 2002], or a structured loss [Taskar and Guestrin, 2003, Tschantz et al., 2004, Bo and Sminchisescu, 2010, Bratieres et al., 2013]. During prediction for a input  $x^* \in \mathcal{X}$ , we search for the best possible label  $y^*$  so that this loss  $\mathcal{L}(f(x^*), y)$  is minimized, given all of training data, and for all possible labels  $y \in \mathcal{Y}$ , such that,

$$y^* = f(x^*) = \arg \min_{y \in \mathcal{Y}} \mathcal{L}(f(x^*), y)$$

In case of kernel methods for structured prediction [Weston et al., 2002, Taskar and Guestrin, 2003, Tschantz et al., 2004, Bo and Sminchisescu, 2010, Schölkopf et al., 2006, Nowozin and Lampert, 2011], space of functions  $\mathcal{H}$  is specified by positive definite kernel functions, which further are jointly defined on the input and output space as  $h((x, y), (x', y'))$ . In the most common case, this kernel is factorized over the input and output domain as  $k(x, x')$  and  $g(y, y')$ , with input and output elements  $x, x' \in \mathcal{X}$  and

$y, y' \in \mathcal{Y}$ , respectively. These individual kernels map arguments data to reproducing kernel Hilbert space (RKHS) or kernel feature spaces. They are denoted by  $\mathcal{K}$  and  $\mathcal{G}$ , respectively. Now, it is well known that performance of kernel algorithms critically depends on the choice of kernel functions ( $k(x, x')$  and  $g(y, y')$ ), and learning them is a challenging problem. In this work, we propose a method to learn kernel feature space representations over input and output data for problem of structured prediction.

Our contributions are as follows, first, we propose to use of monomial and expansion of dot product and Gegenbaur expansion of radial kernel to learn a polynomial combination kernel features over both input and output. Second, we propose an efficient, matrix-based algorithm to solve for these expansions. And third, we show state-of-the art results on synthetic and real-world datasets data using Twin Gaussian Processes of Bo and Sminchisescu [2010] as a prototypical kernel method for structured prediction.

## 1.1 Related work

In the seminal work of Micchelli and Pontil [2005] showed that we can parametrize a family of kernels  $\mathcal{F}$  over a compact set  $\Omega$  as

$$\mathcal{F} = \left\{ \int_{\Omega} G_{\omega}(x) d\omega : p \in \mathcal{P}(\Omega) \right\},$$

where  $\mathcal{P}(\Omega)$  is a set of all probability measures on  $\Omega$ , and  $G(\omega)$  is a base kernel parametrized by  $\omega$ . To illustrate with an example, if we set  $\Omega \subseteq \mathbb{R}_+$  and  $G_{\omega}(x)$  as multivariate Gaussian kernel over  $x$ , with variance  $\omega$ , then  $\mathcal{F}$  corresponds to a subset of the class of radial kernels.

Most kernel learning frameworks in past have focussed on learning a single kernel from a family of kernels ( $\mathcal{F}$ ) defined using above equation. All of these frameworks have focussed on problem of classification or regression. Table 1 illustrates previous work on learning kernels for different choices of  $\Omega$ , and base kernel  $G_{\omega}(x, y)$ , over data domain  $\mathcal{X}$ . Some of the above approaches work iteratively, [Argyriou et al., 2005, 2006]

Kernel family and base kernel $G_{\omega}(x, y)$	Related Work
Radial kernels (Iterative), $G_{\omega}(x, y) = e^{-\omega\ x-y\ ^2}$	Argyriou et al. [2005, 2006].
Dot product kernels, $G_{\omega}(x, y) = e^{\omega\langle x, y \rangle}$	Argyriou et al. [2005, 2006].
Finite convex sum of kernels, SimpleMKL	Rakotomamonjy et al. [2008].
Radial kernels (Semi-infinite Programing, Infinite Kernel Learning)	Gehler and Nowozin [2008]
Shift-invariant kernels (Radial and Anisotropic), $G_{\omega}(x - y)$	Shirazi et al. [2010]

Table 1: Kernel learning frameworks which learn kernels as convex combination of base kernels  $G_{\omega}(x, y)$ .

while others use optimization methods such as, semi-infinite programming [Özögür-Akyüz and Weber, 2010], or QCQP [Shirazi et al., 2010]). A review paper by Suzuki and Sugiyama [2011] surveys many of these works on various Multiple Kernel Learning algorithms. The relevant works which uses results on polynomial expansion of kernels has been of Smola et al. [2000] which learn dot product kernels using monomial basis  $\{1, x, x^2, \dots\}$ , and learning shift-invariant kernels using radial base kernels of Shirazi et al. [2010], both of these have been proposed for classification and regression.

We use results on expansion of kernels for learning kernels for problem of structured regression. In propose a framework to learn kernels for structured prediction that use monomial and Gegenbaur expansions to learn a positive combination of base kernels. The Gegenbaur basis has an advantage of being orthonormal and provides a weight parameter  $\gamma$  that helps avoid Gibbs phenomenon observed in interpolation [Gottlieb et al., 1992].

Outline of this paper is as follows. In section 2 we describe radial and dot product kernels along and their respective polynomial expansions. In section 3 we describe the dependency criteria (HSIC) used in our problem formulation. In section 4 we describe our proposed algorithm. In section 5 we describe Twin Gaussian Processes used for structured prediction. In section 6 we present experimental results on several synthetic and real-world datasets. Finally, section 7 and section 8 are discussion and conclusion, respectively.

## 2 Kernel Transformations

### 2.1 Radial and Dot Product Kernels

A classical result of Schoenberg [1938] states that any continuous, isotropic, kernel  $k(x, x')$ , is positive definite if and only if  $k(x, x') = \phi(\langle x, x' \rangle)$ , and  $\phi(t)$  is a real valued function such that

$$\phi(t) = \sum_{i=0}^{\infty} \alpha_k G_k^\lambda(t), \quad t \in [-1, 1]$$

where  $\sum_{k=0}^{\infty} \alpha_k \geq 0$ ,  $k \in \mathcal{Z}^+$  and  $\alpha_k G_k^\lambda(1) < \infty$ . The symbol  $G_k^\lambda(t)$  stands for what is known as ultraspherical or Gegenbaur basis polynomials. Examples of such kernels include the Gaussian and Laplacian kernels.

To understand this better, if we look at a result of Bochner [1959] which says that, a continuous, shift-invariant kernel  $k(\cdot)$  is positive definite, if and only if, it is a inverse Fourier transform of a finite non-negative probability measure  $\mu$  on  $\mathbb{R}^d$ .

$$k(x - y) = \phi(z) = \int_{\mathbb{R}^d} e^{\sqrt{-1}\langle z, s \rangle} d\mu(s), \quad x, y, s \in \mathbb{R}^d$$

This results allows us to represent a shift-invariant kernel uniquely as a spectral distribution in a spectral domain. Now, if we take the Fourier transform of equation 2.1, we have a unique representation of positive definite kernel  $\phi(t)$ , and also a unique representations of positive definite base kernels  $G_k^\lambda(t)$ ,  $k = 1, 2, \dots$ , in the spectral domain. Hence, the kernel expansion is a nonnegative mixture of base spectral distributions whose kernels are given by kernels  $G_k^\lambda(t)$  with nonnegative weights  $\alpha_k$ 's.

If we look at monomial basis instead of Gegenbaur basis, a similar interpretation can be given for dot product kernels as mentioned in Smola et al. [2000]. Additionally, we know that the span of monomials form a dense basis in  $L_2[-1, 1]$ , and by Weierstrass approximation theorem [Szegő, 1939], any continuous function on a  $[-1, 1]$  can be approximated uniformly on that interval by polynomials to any degree of accuracy. The Gegenbaur basis is orthonormal and provides additional benefits in interpolation accuracy for functions with sharp changes. Thus avoiding the so called Gibbs phenomenon, [Gottlieb et al., 1992].

In our work, we use above expansions of kernel  $k'(\cdot, \cdot)$  on features obtained from an initial kernel  $k(\cdot, \cdot)$ , defined on  $\mathcal{X} \times \mathcal{X}$ . We refer to  $k(\cdot, \cdot)$  as initial kernel, and estimate  $\phi(t)$  which when applied to kernel matrix  $[\mathbf{K}]_{i,j} = \langle x, y \rangle$  gives us a new kernel matrix  $[\mathbf{K}']_{i,j} = \phi([\mathbf{K}]_{i,j})$ . Figure 1 illustrates this pictorially.

### 2.2 Monomial Transformations

In case of the monomial basis functions we have the following expansion.

**Theorem 2.1** (Schoenberg [1938]). *For a continuous function  $\phi: [-1, 1] \rightarrow \mathbb{R}$  and  $k(x, y) = \phi(\langle x, y \rangle)$ , the kernel matrix  $\mathbf{K}'$  defined as  $\mathbf{K}' = \phi([\mathbf{K}]_{i,j})$  is positive definite for any positive definite matrix  $\mathbf{K}$  if and only*

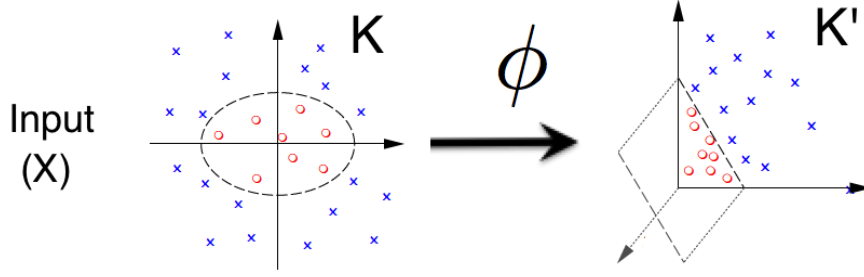


Figure 1: Finding of Kernel Transformations  $\phi(\cdot)$

if  $\phi(\cdot)$  is real entire, and of the form below

$$k'(\langle x, y \rangle) = \phi(t) = \sum_{i=0}^{\infty} \alpha_i t^i \quad (1)$$

with  $\alpha_i \geq 0$  for all  $i \geq 0$ .

So  $\phi(t)$  is an infinitely differentiable and all coefficients  $\alpha_j$  are non-negative (eg.  $\phi(t) = e^t$ ). A benefit of this monomial expansion is that it is easy to compute and can be readily evaluated in parallel.

### 2.3 Gegenbaur Transformations

We obtain Gegenbaur's basis if we insist on having an orthonormal expansion. These expansions are also more general, in the sense that they include a weight function  $w(t; \gamma)$ , which controls the size of the function space used for representation, controlled by a parameter  $\gamma > -1/2$ .

To formally state,

**Theorem 2.2** (Schoenberg [1938]). *For a real polynomial  $\phi: [-1, 1] \rightarrow \mathbb{R}$  and for any finite  $X = \{x_1, x_2, x_3, \dots\}$  the matrix  $[\phi(\langle x_i, x_j \rangle)]_{i,j}$  is positive definite if and only if  $\phi(t)$  is a nonnegative linear combination of Gegenbaur's polynomials  $G_i^\gamma(t)$ , which is,*

$$\phi(t) = \sum_{i=0}^{\infty} \alpha_i G_i^\gamma(t) \quad (2)$$

with  $\alpha_i \geq 0$ , and  $\sum_i \alpha_i G_i^\gamma(1) < \infty$ .

**Definition 2.1.** Gegenbaur's polynomials are defined as below,

$$G_0^\gamma(t) = 1, G_1^\gamma(t) = 2\gamma t, \dots, \quad (3)$$

$$G_{i+1}^\gamma(t) = \left( \frac{2(\gamma + i)}{i + 1} \right) t G_i^\gamma(t) - \left( \frac{2\gamma + i - 1}{i + 1} \right) G_{i-1}^\gamma(t) \quad (4)$$

As stated earlier  $G_k^\gamma$  and  $G_l^\gamma$  are orthogonal in  $[-1, 1]$  and all polynomials are orthogonal with respect to the weight function  $w(t; \gamma) = (1 - t^2)^{(\gamma-1/2)}$  and  $\gamma > -1/2$ .

$$\int_{-1}^1 G_k^\gamma(t) G_l^\gamma(t) w(t; \gamma) dt = 0, \quad k \neq l. \quad (5)$$

The weight function above defines a weighted inner product on the space of functions with a norm and a inner product given by

$$\|\phi\|^2 = \int_{-1}^1 w(t; \gamma) \phi(t) \overline{\phi(t)} dt, \quad (6)$$

$$\langle \phi, \psi \rangle = \int_{-1}^1 w(t; \gamma) \phi(t) \overline{\psi(t)} dt \quad (7)$$

This weight function controls the space of functions over which we estimate these polynomial maps. Figure 2 shows the weight function obtained by different  $\gamma$  parameter. We observe that  $\gamma$  value controls the behavior of the function at the boundary points  $\{1, -1\}$ . Having this weight function also improves the the quality of interpolation by avoiding the Gibbs phenomenon as further explained in Gottlieb et al. [1992].

To summarize given a base kernel matrix  $\mathbf{K}$  on input data, we expand the target kernel  $\mathbf{K}'$  as a transformation  $\phi(t)$  applied to  $\mathbf{K}$ . This maps the initial RKHS features  $k(x, \cdot)$  to new RKHS features  $k'(x, \cdot)$ . These two forms of the polynomial mapping representations have been known before in the literature but have mostly used for non-structured prediction tasks like regression and classification. In our approach, we use these expansions on both input and output kernels so as to maximize dependence between mapped feature spaces  $k'(x, \cdot)$  and  $g'(y, \cdot)$ , using the Hilbert Schmidt Independence Criterion (HSIC) described below.

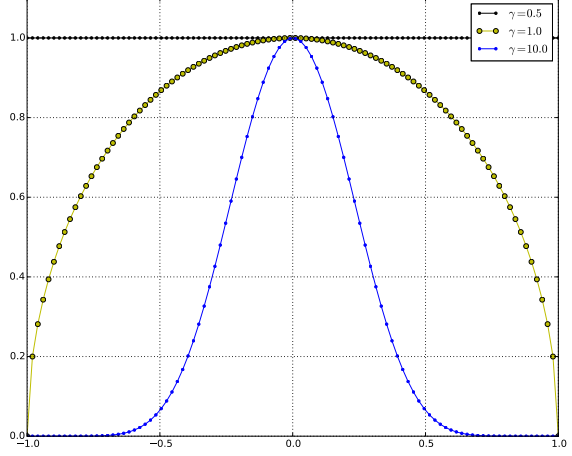


Figure 2: Weight function  $w(t; \gamma)$  as a function of  $\gamma$ , as we see that the  $\gamma$  value controls the behavior of the weight function at the boundaries, and equivalently controlling the size of the function space, which decreases with size.

### 3 Hilbert Schmidt Independence Criterion

To measure cross-correlation or dependence between structured input and output data in kernel feature Gretton et al. [2005] proposed a Hilbert Schmidt Independence criterion (HSIC). Given i.i.d. sampled input-output pair data,  $\{(x_1, y_1), (x_2, y_2), \dots, (x_m, y_m)\} \sim P(x, y)$  HSIC measures the dependence between  $\mathcal{X}$  and  $\mathcal{Y}$ .

**Definition 3.1.** If we have two RKHS's  $\mathcal{K}$  and  $\mathcal{G}$ , then a measure of statistical dependence between  $\mathcal{X}$  and  $\mathcal{Y}$  is given by the norm of the cross-covariance operator  $\mathbf{M}_{xy} : \mathcal{G} \rightarrow \mathcal{K}$ , which is defined as,

$$\mathbf{M}_{xy} := \mathbf{E}_{x,y}[(k(x, \cdot) - \mu_x) \otimes (g(y, \cdot) - \mu_y)] \quad (8)$$

$$= \mathbf{E}_{x,y}[(k(x, \cdot) \otimes g(y, \cdot))] - \mu_x \otimes \mu_y \quad (9)$$

and the measure is given by the Hilbert-Schmidt norm of  $\mathbf{M}_{xy}$  which is,

$$HSIC(p_{xy}, \mathcal{K}, \mathcal{G}) := \|\mathbf{M}_{xy}\|_{HS}^2 \quad (10)$$

So the larger the above norm, the higher the statistical dependence between  $\mathcal{X}$  and  $\mathcal{Y}$ . The advantages of using HSIC for measuring statistical dependence, as stated in Gretton et al. [2005] are as follows: first, it has good uniform convergence guarantees; second, it has low bias even in high dimensions; and third a number of algorithms can be viewed as maximizing HSIC subject to constraints on the labels/outputs. Empirically, in terms of kernel matrices it is defined as

**Definition 3.2.** Let  $Z := \{(x_1, y_1), \dots, (x_m, y_m)\} \subseteq \mathcal{X} \times \mathcal{Y}$  be a series of  $m$  independent observations drawn from  $p_{xy}$ . An unbiased estimator of  $HSIC(Z, \mathcal{K}, \mathcal{G})$  is given by,

$$HSIC(Z, \mathcal{K}, \mathcal{G}) = (m-1)^{-2} \text{trace}(\mathbf{K} \mathbf{H} \mathbf{G} \mathbf{H}) \quad (11)$$

where  $\mathbf{K}, \mathbf{H}, \mathbf{G} \in \mathbb{R}^{m \times m}$ ,  $[\mathbf{K}]_{i,j} := k(x_i, x_j)$ ,  $[\mathbf{G}]_{i,j} := g(y_i, y_j)$  and  $[\mathbf{H}]_{i,j} := \delta_{ij} - m^{-1}$

Now, for well defined *normalized* and *bounded* kernels,  $\mathbf{K}$  and  $\mathbf{G}$ . We have  $HSIC(Z, \mathcal{K}, \mathcal{G}) \geq 0$ . For the ease of discussion we denote  $HSIC(Z, \mathcal{K}, \mathcal{G})$  by  $\overline{HSIC}(\mathbf{K}, \mathbf{G})$ . So we use HSIC to measure dependence between kernels in the target kernel feature space and estimate these transformations  $(\alpha_i's, \beta_j's)$  by maximizing it.

## 4 Learning Kernel Transformations

The goal in structured prediction is to predict output label  $y \in \mathcal{Y}$ , given a input example  $x \in \mathcal{X}$ , our thesis is that if output kernel feature  $g'(y, \cdot)$  is more correlated (dependent) with input kernel feature  $k'(x, \cdot)$ , then we can significantly improve the regression performance. We propose to use HSIC for this. Also, maximizing HSIC (or equivalently Kernel Target Alignment) has been used as an objective for learning kernels in the past [Cortes et al., 2012]. These frameworks maximize the HSIC or alignment between input and outputs, which in our case are structured objects. Shawe-Taylor and Kandola [2002] in their work provide generalization bounds and which confirm that maximizing alignment (i.e HSIC) does indeed lead to better generalization.

Following on this, if we let  $\mathbf{K}' = \phi(\mathbf{K})$ , and  $\mathbf{G}' = \psi(\mathbf{G})$ , where  $\mathbf{K}$  and  $\mathbf{G}$  are normalized base kernels on input and output data. Using the empirical definition  $\overline{HSIC}$  we define the following objective function to optimize as,

$$\mathbf{L}(\alpha*, \beta*) = \max_{\alpha, \beta} \overline{HSIC}(\phi(\mathbf{K}), \psi(\mathbf{G})) \quad (12)$$

$$\text{subject to } \alpha_i \geq 0, \beta_j \geq 0, \forall i, j \geq 0 \quad (13)$$

In case of monomial basis as in section 2.2, we can use equation 1 on kernel matrices  $\mathbf{K}$  and  $\mathbf{G}$  we get equations for  $\phi : \mathbf{K} \rightarrow \mathbf{K}'$  and  $\psi : \mathbf{G} \rightarrow \mathbf{G}'$  as follows,

$$\phi(\mathbf{K}) = \sum_{i=0}^{\infty} \alpha_i \mathbf{K}^{(i)}, \alpha_i \geq 0, \forall i \geq 0 \quad (14)$$

$$\psi(\mathbf{G}) = \sum_{j=0}^{\infty} \beta_j \mathbf{G}^{(j)}, \beta_j \geq 0, \forall j \geq 0 \quad (15)$$

where  $\mathbf{K}^{(i)}$  is the kernel obtained by applying the  $i^{th}$  polynomial basis  $t^i$ , to the base kernel matrix  $\mathbf{K}$  (similarly  $G_k^\lambda(t)$  for Gegenbaur basis). Figure 3 illustrates this. Assuming our base kernels are both bounded and normalized we also need our new kernels  $\phi(\mathbf{K})$  and  $\psi(\mathbf{G})$  to be at-least bounded. For this purpose, we impose  $l_2$ -norm regularization constraint on  $\alpha_i$ 's and  $\beta_j$ 's, that is  $\|\alpha\|^2 = 1$  and  $\|\beta\|^2 = 1$ . These constraints are similar to the  $l_2$ -norm regularization constraint on positive mixture coefficient's in the Multiple Kernel

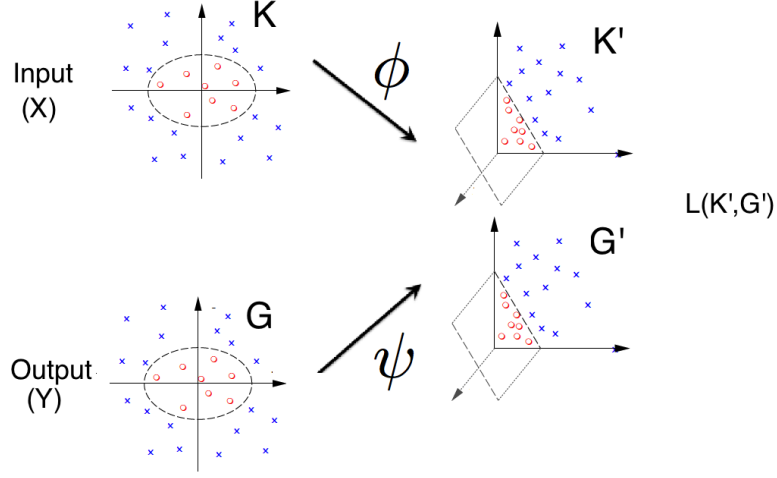


Figure 3: Twin Kernel Learning

Learning framework of Cortes et al. [2012]. These helps generalization to unseen test data and also avoid arbitrary increase of optimization objective so as to maximize it.

Substituting the expansions equations 14 and 15 in equation 13, and simplifying the main objective 13 and we get,

$$\begin{aligned} & \text{maximize } \sum_{i=0}^{\infty} \sum_{j=0}^{\infty} \alpha_i \beta_j \mathbf{C}_{i,j} \\ & \text{subject to, } \|\alpha\|_2 = 1, \|\beta\|_2 = 1 \end{aligned} \quad (16)$$

where the  $\mathbf{C}$ -matrix is such that  $[\mathbf{C}]_{i,j} = \overline{HSIC}(\mathbf{K}^{(i)}, \mathbf{G}^{(j)})$ . Also, we know that the entries of the  $\mathbf{C}$ -matrix are non-negative. The  $\mathbf{C}$ -matrix looks as follows,

$$\mathbf{C} = \begin{array}{c|cccc} & K^{(0)} & K^{(1)} & K^{(i)} & K^{(d_2)} \\ \hline G^{(0)} & C_{1,1} & C_{1,2} & \vdots & C_{d_2,1} \\ G^{(1)} & C_{1,1} & C_{1,2} & \vdots & C_{d_2,1} \\ G^{(0)} & C_{2,1} & C_{1,2} & \vdots & C_{2,d_2} \\ G^{(j)} & \dots & \dots & C_{i,j} & \dots \\ G^{(d_1)} & C_{d_1,1} & C_{d_1,2} & \vdots & C_{d_1,d_2} \end{array} \quad (17)$$

where  $C_{i,j} = \overline{HSIC}(\mathbf{K}^{(i)}, \mathbf{G}^{(j)})$ .

To further explain, every entry  $[\mathbf{C}]_{i,j} = \overline{HSIC}(\mathbf{K}^{(i)}, \mathbf{G}^{(j)})$  represents higher order cross-correlations among the polynomial combination of features of order  $i$  and  $j$  between input and output, respectively. Hence by appropriately choosing coefficient's  $\alpha_i$  and  $\beta_j$  we are maximizing these higher order cross-correlations in the target kernel feature space. Here we approximate sum to finite degrees  $d_1$  and  $d_2$  which leads us to a finite dimensional problem with  $\deg(\phi) = d_1$  and  $\deg(\psi) = d_2$ . This amounts to using all polynomial combinations of features up to degree  $d_1$  for input and  $d_2$  for output. So higher the degree we choose more

is the dependence and intuitively better is the prediction. The upper bound on the degree is computationally limited by the added non-linearity in the kernel based prediction algorithm and can lead to overfitting. So we choose these degrees empirically by cross-validation until we saturate the performance of the prediction algorithm.

We have the following theorem regarding the solution of optimization problem 16,

**Theorem 4.1.** *The solution  $(\alpha^*, \beta^*)$  to the optimization problem in 16 is given by the first left and right singular vector of the  $\mathbf{C}$ -matrix*

*Proof.* Using Perron-Frobenius theorem [Chang et al., 2008] for square non-negative matrices  $\mathbf{C}^T \mathbf{C}$  and  $\mathbf{C} \mathbf{C}^T$ , we claim that both  $\mathbf{C}^T \mathbf{C}$  and  $\mathbf{C} \mathbf{C}^T$  have Perron vectors  $\alpha^*$  and  $\beta^*$ , respectively. Both  $\alpha^*$  and  $\beta^*$  are the left and right singular vectors of  $\mathbf{C}$  and also maximize Eq. 16.  $\square$

This above theorem gives us our required solution to the problem. Hence, to solve for the unknown's  $\alpha_i$ 's and  $\beta_j$ 's we do Singular Value Decomposition (SVD) of the  $\mathbf{C}$ -matrix and choose  $\alpha$  and  $\beta$  to be the first left and right singular vectors Theorem 4.1. The non-negativity of the  $\alpha$  and  $\beta$  vector is guaranteed due to non-negativity of the  $\mathbf{C}$ -matrix combined with Perron-Frobenius theorem Chang et al. [2008].

We also observe that  $\alpha_0 = \beta_0 = 0$ , so choosing  $d_1 = 1$  corresponds to using the identity mapping  $\phi(t) = t$  on the input kernel, which corresponds to using the initial kernel only, or equivalently, no mapping on input kernel. A similarly logic also applies if we set  $d_2 = 1$ , then we have  $\psi(t) = t$  and no mapping on output base kernel. This is interesting because if we set  $d_2 = 1$  and  $d_1$  to be some arbitrary value greater than one, then solution  $\alpha^*$  is exactly where  $\alpha_i^* \propto \overline{HSTC}(\mathbf{K}^{(i)}, \mathbf{G})$ , which same as choosing coefficients based on kernel alignment as in Cortes et al. [2012].

We also like to point out the similarity of our proposed objective to that of Kernel Canonical Correlation Analysis (KCCA) objective, which also uses HSIC [Chang et al., 2013]. In KCCA we find two nonlinear mappings  $\phi(\cdot) \in \mathcal{K}$  and  $\psi(\cdot) \in \mathcal{G}$  from their prespecified RKHS's maximizing statistical correlation. In our approach, we also look for analytical kernel transformations  $\phi(\cdot)$  and  $\psi(\cdot)$  on initial kernel matrices to maximize the same objective.

## 5 Twin Gaussian Processes

Twin Gaussian Processes (TGP) of Bo and Sminchisescu [2010], are a recent and popular form of structured prediction methods, which model input-output domains using Gaussian processes with covariance functions, represented by  $\mathbf{K}$  and  $\mathbf{G}$ . These covariance matrices encode prior knowledge about the underlying process that is being modeled. In many real world applications data is high dimensional and highly structured, and the choice of kernel functions is not obvious. In our work, we aim to learn kernel covariance matrices simultaneously. We use TGP as an illustrative example to demonstrate the benefits of learning them. Although we note that this framework is not limited only to the use of Twin Gaussian Processes.

In TGP choice of the auxiliary evaluation function is typically some form of information measure, e.g. KL-Divergence or HSIC which are known to be special cases of Bregman divergences (See Banerjee et al. [2005]). KL-Divergence is an asymmetric measure of information, while HSIC is symmetric in its arguments. We refer to two versions of Twin Gaussian Processes below corresponding to each of these measures of information. We refer to them as TGP with KL-Divergence or simply TGP, and TGP with HSIC for TGP.

**TGP with KL-Divergence:** In this version of TGP, we minimize the KL-divergence between the kernels,  $\mathbf{K}$  and  $\mathbf{G}$ , given the training data  $\mathcal{X} \times \mathcal{Y}$  and test example  $x^*$ . The prediction function for HOTGP is,

$$y^* = \arg \min_y D_{KL}((\mathbf{G}_{Y \cup y} || \mathbf{K}_{X \cup x^*})) \quad (18)$$



**TGP with HSIC:** For this version of TGP with HSIC criteria, the prediction function maximizes the HSIC between the kernels  $\mathbf{K}$  and  $\mathbf{G}$  given the training data  $(\mathcal{X} \times \mathcal{Y})$ , and test example  $x^*$ . The prediction function looks as follows,

$$y^* = \arg \max_y \overline{HSIC}(\mathbf{G}_{Y \cup y}, \mathbf{K}_{X \cup x^*}) \quad (19)$$

## 5.1 Modified Twin Gaussian Processes (TGP)

We also both of these criteria propose above against degree of mapping  $d_1$  and  $d_2$ . This allows us to show how each information measure is affected as the mapping degrees  $d_1$  and  $d_2$  are increased. The relationship we observe is straightforward and direct, allowing the choice of  $d_1$  and  $d_2$  to be made easily. We refer to these new modified TGP's as Higher Order TGP with KL-Divergence (HOTGP) and Higher Order HSIC (HOHSIC) for TGP using HSIC.

**Modified TGP with KL-Divergence:** In this version of TGP, we minimize the KL-divergence between the transformed kernels,  $\phi(\mathbf{K})$  and  $\psi(\mathbf{G})$ , given the training data  $\mathcal{X} \times \mathcal{Y}$ , and test example  $x^*$ . The prediction function for HOTGP is,

$$\mathbf{y}^* = \arg \min_y D_{KL}((\psi(\mathbf{G}_{Y \cup y}) || \phi(\mathbf{K}_{X \cup x^*})) \quad (20)$$

**Modified TGP with HSIC:** For this version of TGP with HSIC criteria, the prediction function maximizes the HSIC between the transformed kernels  $\phi(\mathbf{K})$  and  $\psi(\mathbf{G})$  given the training data  $\mathcal{X} \times \mathcal{Y}$ , and test example  $x^*$ . The prediction function looks as follows,

$$\mathbf{y}^* = \arg \max_y \overline{HSIC}((\psi(\mathbf{G}_{Y \cup y}), \phi(\mathbf{K}_{X \cup x^*})) \quad (21)$$

## 6 Experiments

We show empirical results using Twin Gaussain Processes with KL-Divergence and HSIC, and using both monomial and Gegenbaur transformations on synthetic and real-world datasets. To measure improvement in performance over the baseline we look at empirical reduction in error which we call *% Gain* defined as

$$\% \text{ Gain} = \left( 1 - \frac{Error_{(mapping)}}{Error_{(no \ mapping)}} \right) \times 100.$$

In all our experiments, we use Gaussian kernels  $k(x_i, x_j) = \exp(-\gamma_x ||x_i - x_j||^2)$  and  $g(y_i, y_j) = \exp(-\gamma_y ||y_i - y_j||^2)$  as base kernels on input and output, respectively. The bandwidth parameters  $\gamma_x$  and  $\gamma_y$  were chosen using cross-validation using base kernel on the original dataset. The weight parameters were chosen to be  $\lambda_1 = 0.51$  and  $\lambda_2 = 0.52$  using rough estimates from expressions in Gottlieb et al. [1992] and validated on validation set. For choice of expansion degree we increase degrees  $d_1$  and  $d_2$  until *% Gain* saturates on the cross-validation. We learn kernel transformations  $\phi(\cdot)$  and  $\psi(\cdot)$  using above proposed approach.

### 6.1 Datasets

#### 6.1.1 Synthetic Data

**S Shape Dataset:** The S-shape synthetic dataset from Dalal and Triggs [2002] is a simple 1D input/output regression problem. In this dataset, 500 values of inputs ( $x$ ) are sampled uniformly in  $(0, 1)$ , and evaluated for  $r = x + 0.3\sin(2\pi x) + \epsilon$  with  $\epsilon$  drawn from a zero mean Gaussian noise with standard deviation  $\sigma = 0.05$  (Figure 4). Goal here is to solve the inverse problem which is to predict  $x$ , given  $r$ . This dataset is challenging in the sense that it is multivalued (in the middle of the S-shape), discontinuous (at the boundary of uni-valued and multivalued region), and noisy ( $\epsilon = \mathcal{N}(0, \sigma)$ ). The error metric used is mean absolute error (MAE).

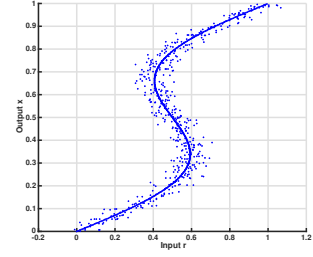


Figure 4: S-Shape dataset.

**Poser Dataset:** Poser dataset contains synthetic images of human motion capture sequences from Poser 7 SmithMicro Software. These motion capture sequences includes 8 categories: walk, run, dance, fall, prone, sit, transitions and misc. There are 1927 training examples coming from different sequences of varying lengths and the test set is a continuous sequence of 418 time steps. Input feature vectors are 100d silhouette shape descriptors while output feature vectors are 54d vectors with  $x, y$  and  $z$  rotation of joint angles. Error metric is mean absolute error (MAE) in mm.

### 6.1.2 Real-world data

**USPS Handwritten Digits Reconstruction** (Figure 5): In USPS handwritten digit reconstruction dataset from Weston et al. [2002] our goal is to predict 16 pixel values at center of an image given outer pixels. We use 7425 examples for training (without labels) and 2475 examples (roughly 1/4th for each digit) for testing. Error metric here is reconstruction error measured using mean absolute error (MAE).

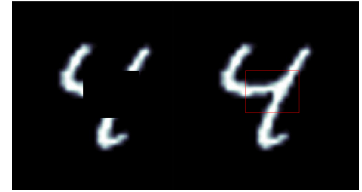


Figure 5: USPS digits.

**HumanEva-I Pose Dataset** (Figure 6): HumanEva-I dataset from Sigal and Black [2006] is a challenging dataset that contains real motion capture sequences from three different subjects (S1,S2,S3) performing five different actions (Walking, Jogging, Box, Throw/Catch, Gestures). We train models on all subjects and all actions. We have input images from three different cameras; C1,C2 and C3 and we use HoG features from Dalal and Triggs [2005] on them. The output vectors are 60d with the  $x, y, z$  joint positions in mm. We report results using concatenated features from all three cameras (C1+C2+C3) and also individual features from each individual camera (C1,C2 or C3).

## 6.2 Results

### 6.2.1 Synthetic data

**S-shape data:** We choose bandwidth parameter to be  $\gamma_x = 1$  and  $\gamma_y = 1$  using cross-validation. To illustrate effect of increasing degrees  $d_1$  and  $d_2$ , we run our results on a grid of degrees from the set  $\{1, 2, 3, 5, 7, 11\}$ . In figure 7 we plot increase in mapping degree as % Gain. Figures 7a and 7b show results for using KL-Divergence as optimization criteria. Figures 7c and 7d show results for using HSIC as an optimization criteria. We observe that for both as we increase  $d_1$  and  $d_2$ , % Gain increases i.e. mean absolute error (MAE) reduces. Also for each pair of figures, for each objective, changing from a monomial basis to Gegenbauer basis helps improve % Gain from 31.27% to 39.49% for KL-Div, and 22.31% to 26.06% for HSIC.

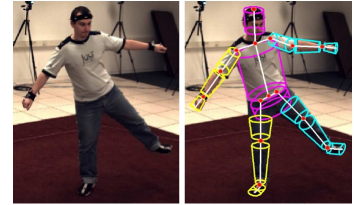
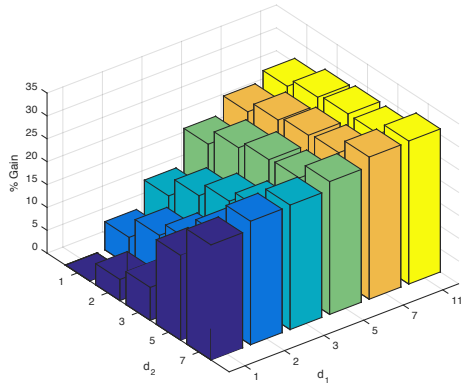
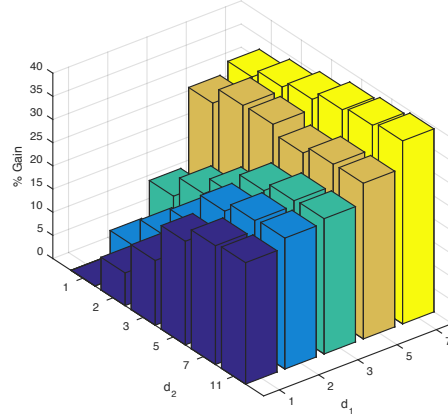


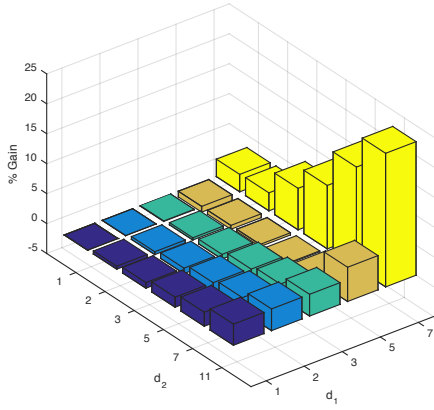
Figure 6: HumanEva-I



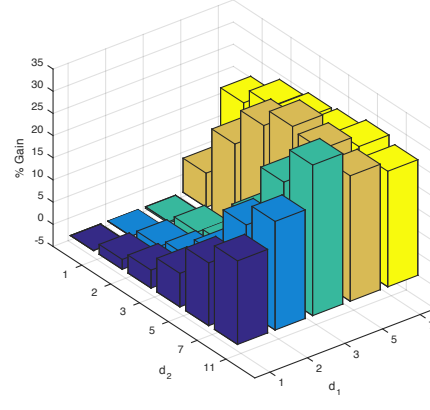
(a) TGP (KL-Div) with Monomial Basis



(b) TGP (KL-Div) with Gegenbaur Basis



(c) TGP (HSIC) with Monomial Basis



(d) TGP (HSIC) with Gegenbaur Basis

Figure 7: % Gain for TGP with KL-Div figures 7a and 7b and HSIC (Figures 7c and 7d) using monomial and Gegenbaur basis on left and right, respectively.

Criterion	$(d_1, d_2)$	MAE (w/o map)	MAE (w/map)	Gain %
KL-Div	(1,11)	57.03	41.57	<b>27.25%</b>
HSIC	(1,11)	48.08	38.71	<b>19.48%</b>
KL-Div (Gegen.)	(1,11)	57.02	44.19	<b>22.50%</b>
HSIC (Gegen.)	(1,23)	48.08	35.55	<b>36.02%</b>

Table 2: Root Mean Absolute Error for the Poser dataset for the two criteria's of TGP using monomial and Gegenbaur transformation.

Method	$(d_1, d_2)$	MAE	Method	$(d_1, d_2)$	MAE
NN	/	0.341	KRR	/	0.250
SVR	/	0.250	KDE	/	0.260
$SOAR_{krr}$	/	0.233	$SOAR_{svr}$	/	0.230
HSIC	(1,1)	0.3399	HSIC	(11,11)	0.195 ( <b>2.50%</b> )
KL-Div	(1,1)	0.2151	KL-Div	(11,11)	0.211 (2.01)%
KL-Div Gegen.	(1,1)	0.2101	KL-Div Gegen.	(11,11)	0.19 ( <b>7.01%</b> )
HSIC Gegen.	(1,1)	0.3399	HSIC Gegen.	(23,23)	0.25442 (25.14%)

Table 3: Comparison with others models from Bo and Sminchisescu [2009] for USPS digits reconstruction dataset. The two lowest errors are *emphasized* and their *% Gain* **bolded**. NN means nearest neighbor regression, KDE means kernel dependency estimation [Weston et al., 2002] with 16d latent space obtained by kernel principal component analysis. SOAR means Structured Output Associative regression [Bo and Sminchisescu, 2009]. Note: The *% Gain* show reduction in error compared to no-mapping vs. using mapping for KL-Div and HSIC criteria and with monomial and Gegenbaur basis.

**Poser:** For Poser dataset we choose bandwidth to be  $\gamma_x = 10$  and  $\gamma_y = 10^{-5}$  using cross-validation. The final results are shown in Table 2. In this case we observe that for both basis input degree turns out be  $d_1 = 1$ , and using Gegenbaur basis gives us better results of 57.02% at  $d_2 = 11$ , when compared to monomial basis with 48.08% at  $d_2 = 23$ . Here we distinctly observe benefits of using Gegenbaur basis in terms better accuracy and better numerical stability with a lower output degree  $d_2$ .

### 6.2.2 Real-world data

**Handwriting Recognition:** We report our results with bandwidth parameters  $\gamma_x = 2e10^{-7}$  and  $\gamma_y = 2e10^{-2}$ . The mapping degrees were chosen for HOTGP were  $(d_1, d_2) = (11, 11)$  and for HOHSIC were  $(d_1, d_2) = (23, 23)$ , using cross validation on MAE criteria. Table 3 shows summary of results and compares our approach with other kernel-based structured prediction methods. We observe two lowest scores to be from Twin Gaussian process using HSIC with monomial basis,  $(d_1, d_2) = (11, 11)$ , and KL-Divergence with Gegenbaur basis,  $(d_1, d_2) = (23, 23)$ . *% Gain* shows that using Gegenbaur basis leads to better same results for lower degree over baseline with no-mapping. Best accuracy is obtained for both objective criteria.

**HumanEva-I Pose Dataset:** We report results using concatenated features from all three cameras (C1+C2+C3), and also features from individual camera (C1, C2 and C3). We use Gaussian kernel with  $\gamma_x = \gamma_y = 10^{-4}$ . For KL-divergence criteria we get  $(d_1, d_2) = (1, 11)$  for monomial basis, and  $(d_1, d_2) = (1, 5)$  for Gegenbaur basis. In case of HSIC criteria, we get  $(d_1, d_2) = (11, 11)$  for both monomial and Gegenbaur basis. Table 4) shows complete set of results. *% Gain* for each criteria is shown in bold. We observe in both subtables that using concatenated features (C1+C2+C3) gives us better results than using individual camera features.

In subtable 4a, we see results with monomials basis for both HSIC KL-Divergence criterion. In general we observe KL-Divergence to be giving better results compared to HSIC. The best results for this case is with features (C1+C2+C3) with KL-Divergence and *% Gain* of 5.080%. In subtable 4b for the Gegenbaur basis we observe a significant reduction in error when using KL-divergence with *% Gain* of 99.95%. We show consistent improvement in performance with this expansion and much better results using Gegenbaur expansion. We provide detailed results on all subjects and actions in appendix.

Features	Crit.	w/map	wo/map	% Gain
HoG (C1C2C3)	KL-Div	45.17	42.88	<b>5.08%</b>
	HSIC	172.66	172.59	<b>0.05%</b>
HoG (C1)	KL-Div	34.29	33.43	<b>2.51%</b>
	HSIC	172.66	173.88	<b>0.08%</b>
HoG (C2)	KL-Div	31.99	31.58	<b>1.29%</b>
	HSIC	172.66	173.88	<b>0.09%</b>
HoG (C3)	KL-Div	30.93	30.49	<b>1.41 %</b>
	HSIC	172.66	172.59	<b>0.09%</b>

(a) Monomial transformation: KL-Div -  $(d_1, d_2) = (1, 11)$ , HSIC- $(d_1, d_2) = (11, 11)$

Features	Crit.	w/map	wo/map	% Gain
HoG (C1C2C3)	KL-Div	25.40	0.011	<b>99.95 %</b>
	HSIC	172.66	172.29	<b>0.25%</b>
HoG (C1)	KL-Div	44.42	9.63	<b>77.46%</b>
	HSIC	172.66	172.28	<b>0.26%</b>
HoG (C2)	KL-Div	44.68	12.30	<b>71.71%</b>
	HSIC	172.66	172.27	<b>0.26%</b>
HoG (C3)	KL-Div	44.35	0.01	<b>99.97%</b>
	HSIC	172.66	172.28	<b>0.26%</b>

(b) Gegenbaur transformation: KL-Div- $(d_1, d_2) = (1, 5)$ , HSIC- $(d_1, d_2) = (11, 11)$

Table 4: Mean Absolute Error for HumanEva-I dataset for the two criteria KL-Div and HSIC with and without mapping using both monomials transformation and Gegenbaur transformation.

## 7 Discussion

% Gain	Criterion	S-shape	Poser	USPS Digits	HumaEva-I (C1+C2+C3)	HumanEva-I (C1,C2,C3)
	KL-Div.	31.27 %.	6.39 %	1.97 %	5.08%	(2.51%, 1.29%, 1.40%)
	HSIC	22.31 %.	1.26%	2.11 %	0.05%	(0.08%, 0.09%, 0.09%)
	KL-Div. (Gegen.)	39.49 %.	14.31%	14.31 %	99.95 %	(77.46%,71.71% 99.97%)
	HSIC (Gegen.)	26.06 %.	7.01%	7.01 %	0.25 %	(0.26%,0.26%, 0.26%)

Table 5: % Gain for all datasets with both criteria, and using both monomial and Gegenbaur transformation.

Table 5 provides a complete summary of results for all datasets. It is clear from experimental results that as we increase mapping degrees  $d_1$  and  $d_2$ , we use higher order combination of polynomial kernel features to maximize dependence between input and output, and this leads to better regression. Reduction in prediction error as indicated by the % Gain metric. Choice of degree is done using cross-validation and kernel parameters are selected using the kernel median trick. In S-shape dataset increase in both  $d_1$  and  $d_2$  helps until the performance saturates, and later falls off due to numerical instability due to the added non-linearity and overfitting.

For the case of the Poser dataset (Table 2) and for HumanEva with KL-Divergence (Table 4a and 4b), we see that the best performance is for  $d_1$  equal to one. This amounts to choosing the identity mapping/no-mapping on input,  $\phi(t) = t$ . As we described in section 4 this amounts to choosing coefficients proportional to kernel target alignment of Cortes et al. [2012] score between initial input kernel and kernels obtained from basis expansion of initial output kernel  $\mathbf{G}$ .

The effect of using the two different objective criteria KL-Divergence versus HSIC, we see that in many cases, KL-Divergence does better or as well as HSIC (Table 3). In terms of ease of optimization of TGP with HSIC, it turns out to be easier criteria to optimize as there is no explicit training step for it [Bo and Sminchisescu, 2010], and it is relatively easier to compute objective than KL-Divergence.

In terms of choice of basis functions, it is clear that using Gegenbaur basis leads to better numerical

stability and often times better results. In some cases like HumaEva with KL-Divergence (Table 4b), it does lead to using lower degree values and leads to easier optimization during prediction in TGP.

## 8 Conclusions and Future Work

We proposed a novel method for learning kernels using polynomial expansions of base kernels. We empirically showed that maximizing dependency between input and output kernel features leads to better performance in structured prediction. We propose an efficient matrix-decomposition based algorithm to learn these kernel transformations. We show state-of-the-art empirical results using Twin Gaussian Processes on several synthetic and real-world datasets.

For future work, we plan to further investigate; 1) automated learning of kernel parameters  $d_1, d_2$  and  $\gamma$  by using distributional priors on them and optimizing for data likelihood, 2) extending this framework to multiple kernels for multi-modal and/or multi-task prediction, and 3) joint learning of kernels and prediction.

## References

- Andreas Argyriou, Charles A Micchelli, and Massimiliano Pontil. Learning Convex Combinations of Continuously Parameterized Basic Kernels. *Conference on Learning Theory*, 3559(23):338–352, 2005.
- Andreas Argyriou, Raphael Hauser, Charles A Micchelli, and Massimiliano Pontil. A DC-programming algorithm for kernel selection. *International Conference on Machine Learning*, pages 41–48, 2006.
- Arindam Banerjee, Srujana Merugu, Inderjit S Dhillon, and Joydeep Ghosh. Clustering with Bregman divergences. 6:1705–1749, 2005.
- Liefeng Bo and C Sminchisescu. Structured output-associative regression. In *IEEE Conference on Computer Vision and Pattern Recognition Workshops*, pages 2403–2410. IEEE, June 2009.
- Liefeng Bo and Cristian Sminchisescu. Twin Gaussian Processes for Structured Prediction. *IEEE Conference on Computer Vision and Pattern Recognition*, 87(1-2):28–52, 2010.
- Salomon Bochner. *Lectures on Fourier Integrals*. Princeton University Press, 1959.
- Sebastien Bratieres, Novi Quadrianto, and Zoubin Ghahramani. Bayesian Structured Prediction Using Gaussian Processes. July 2013.
- Billy Chang, Uwe Kruger, Rafal Kustra, and Junping Zhang. Canonical Correlation Analysis based on Hilbert-Schmidt Independence Criterion and Centered Kernel Target Alignment. pages 316–324, 2013.
- K. C. Chang, K. Pearson, and T. Zhang. Perron-Frobenius theorem for nonnegative tensors. *Communications in Mathematical Sciences*, 6(2):507–520, June 2008.
- Corinna Cortes, Mehryar Mohri, and Afshin Rostamizadeh. Algorithms for Learning Kernels Based on Centered Alignment. (1):550–828, March 2012.
- Navneet Dalal and Bill Triggs. Histograms of oriented gradients for human detection. *2005 IEEE Computer Society Conference on Computer Vision and Pattern Recognition (CVPR’05)*, 1:886–893 vol. 1, August 2002.
- Navneet Dalal and Bill Triggs. Histograms of Oriented Gradients for Human Detection. *IEEE Conference on Computer Vision and Pattern Recognition*, 1:886–893, 2005.

- Peter Gehler and Sebastian Nowozin. Infinite kernel learning. 2008.
- David Gottlieb, Chi-Wang Shu, Alex Solomonoff, and Hervé Vandeven. On the Gibbs phenomenon. I. Recovering exponential accuracy from the Fourier partial sum of a nonperiodic analytic function. *Journal of Computational and Applied Mathematics*, 43(1-2):81–98, 1992.
- Arthur Gretton, Olivier Bousquet, Alexander J Smola, and Bernhard Schölkopf. Measuring Statistical Dependence with Hilbert-Schmidt Norms. *ALT*, 3734(Chapter 7):63–77, 2005.
- Charles A Micchelli and Massimiliano Pontil. Learning the Kernel Function via Regularization. pages 1099–1125, 2005.
- Sebastian Nowozin and Christoph H Lampert. Structured Learning and Prediction in Computer Vision. *Foundations and Trends in Computer Graphics and Vision* (), 6(3-4):185–365, 2011.
- Süreyya Özögür-Akyüz and Gerhard-Wilhelm Weber. On numerical optimization theory of infinite kernel learning. *Journal of Global Optimization*, 48(2):215–239, 2010.
- Alain Rakotomamonjy, Francis R Bach, Stéphane Canu, and Yves Grandvalet. SimpleMKL. *The Journal of Machine Learning Research*, 9:2491–2521, 2008.
- Isaac Jacob Schoenberg. Metric Spaces and Completely Monotone Functions. *The Annals of Mathematics*, 39(4):811, October 1938.
- Bernhard Schölkopf, Alexander J Smola, Ben Taskar, and SVN Vishwanathan. Predicting Structured Data. Technical report, 2006.
- N Shawe-Taylor and A Kandola. On kernel target alignment. 14:367, 2002.
- Sayed Kamaledin Ghiasi Shirazi, Reza Safabakhsh, and Mostafa Shamsi. Learning Translation Invariant Kernels for Classification. *Journal of Machine Learning Research*, 11:1353–1390, 2010.
- L Sigal and M J Black. Humaneva: Synchronized video and motion capture dataset for evaluation of articulated human motion. 2006.
- SmithMicro Software. Poser 3D Animation & Character Creation Software . URL <http://poser.smithmicro.com/>.
- Alexander J Smola, Zoltán L Óvári, and Robert C Williamson. Regularization with Dot-Product Kernels. *Advances in neural information processing systems*, pages 308–314, 2000.
- Taiji Suzuki and Masashi Sugiyama. Multiple Kernel Learning Algorithms. *Journal of Machine Learning Research*, pages 2211–2268, 2011.
- Gabor Szegő. *Orthogonal Polynomials*. American Mathematical Soc., 1939.
- Ben Taskar and Carlos Guestrin. Max-Margin Markov Networks. In *Advances in neural information processing systems*, 2003.
- Ioannis Tsochantaridis, Thomas Hofmann, Thorsten Joachims, and Yasemin Altun. Support vector machine learning for interdependent and structured output spaces. *ICML 2004*, page 104, 2004.
- Jason Weston, Olivier Chapelle, Vladimir Vapnik, Andre Elisseeff, and Bernhard Schölkopf. Kernel dependency estimation. pages 873–880, 2002.

## A Perron-Frobenius

**Theorem A.1** (Perron O., Frobenius G. (1912) ). For  $\mathbf{A}_{n \times n} \geq 0$ , with spectral radius  $r = \rho(\mathbf{A})$ , the following statements are true.

1.  $r \in \sigma(\mathbf{A})$  and  $r > 0$
2.  $r$  is unique and it the spectral radius of  $\mathbf{A}$
3.  $\mathbf{A}\mathbf{z} = r\mathbf{z}$  for some  $\mathbf{z} \in \Delta^n = \{\mathbf{x} | \mathbf{x} \geq 0 \text{ with } \mathbf{x} \neq \mathbf{0}\}$
4. There is unique vector defined by

$$\mathbf{A}\mathbf{p} = r\mathbf{p}, \mathbf{p} > 0, \text{ and } \|\mathbf{p}\|_1 = 1, \quad (22)$$

is called **Perron vector** of  $\mathbf{A}$  and there are no other nonnegative vectors except for positive multiples of  $\mathbf{p}$ , regardless of eigenvalue.

## B Kernel gradients

For data points  $X = \{x_1, x_2, \dots, x_m\}$  and test data point  $x$ .

$$\frac{\partial \phi(K(x_1, x))}{\partial x^{(d)}} = \frac{\partial \phi(t)}{\partial t} \Big|_{t=K(x_1, x)} \frac{\partial K(x_1, x)}{\partial x^{(d)}}$$

$$\frac{\partial \phi(t)}{\partial t} = \sum_{i=0}^{d_1} \alpha_i H_i^\gamma(t)$$

$$H_0^\gamma(t) = 0, H_1^\gamma(t) = 2\gamma, \quad (23)$$

$$H_{i+1}^\gamma(t) = \left( \frac{2(\gamma + i)}{i + 1} \right) (tH_i^\gamma(t) + G_i^\gamma(t)) - \left( \frac{2\gamma + i - 1}{i + 1} \right) H_{i-1}^\gamma(t) \quad (24)$$

$$\frac{\partial \phi(K(X, x))}{\partial x^{(d)}} = \begin{bmatrix} \frac{\partial \phi(t)}{\partial t} \Big|_{t=K(x_1, x)} \frac{\partial K(x_1, x)}{\partial x^{(d)}} \\ \frac{\partial \phi(t)}{\partial t} \Big|_{t=K(x_2, x)} \frac{\partial K(x_2, x)}{\partial x^{(d)}} \\ \vdots \\ \frac{\partial \phi(t)}{\partial t} \Big|_{t=K(x_m, x)} \frac{\partial K(x_m, x)}{\partial x^{(d)}} \end{bmatrix}$$

### B.1 RBF kernel

$$K(x_i, x_j) = e^{-\gamma \|x_i - x_j\|^2}$$

$$\frac{\partial K(X, x)}{\partial x^{(d)}} = \begin{bmatrix} -2\gamma(-x_1^{(d)} + x^{(d)})K(x, x_1) \\ -2\gamma(-x_2^{(d)} + x^{(d)})K(x, x_2) \\ \vdots \\ -2\gamma(-x_m^{(d)} + x^{(d)})K(x, x_m) \end{bmatrix}$$

$$\frac{\partial K(x_1, x)}{\partial x^{(d)}} = -2\gamma(-x_1^{(d)} + x^{(d)})K(x, x_1)$$



## B.2 Linear kernel

$$K(x_i, x_j) = \gamma \langle x_i, x_j \rangle$$

$$\frac{\partial K(X, x)}{\partial x^{(d)}} = \begin{bmatrix} \gamma x_1^{(d)} \\ \gamma x_2^{(d)} \\ \vdots \\ \gamma x_m^{(d)} \end{bmatrix}$$

## C Additional Results

Crit. / Mean Abs. Er	(no mapping)	(mapping)	Gain %
KL-Div (11,11)	0.2151	0.21078	<b>2.008 %</b>
HSIC (11,11)	0.3399	0.19536	<b>2.5007 %</b>
KL-Div (Gegen.) (11,11)	0.2101	0.19536	<b>7.0096 %</b>
HSIC (Gegen.) (23,23)	0.3399	0.25442	<b>25.1441 %</b>

Table 6: Mean Absolute Error for *USPS Handwritten digits* dataset for the two criteria, with and without mapping.

Features	Motions	Subject 1			Subject 2			Subject 3		
		TGP	HOTGP	% Gain	TGP	HOTGP	% Gain	TGP	HOTGP	% Gain
HoG (C1C2C3)	Walking	41.0491	38.0943	<b>7.1984</b>	27.3651	25.1213	<b>8.1998</b>	49.5457	46.8701	<b>5.4003</b>
	Jog	48.3995	47.1128	<b>2.6585</b>	37.7046	35.4643	<b>5.9417</b>	39.8883	37.3239	<b>6.4288</b>
	Gestures	16.3853	14.5804	<b>11.0155</b>	46.6891	44.3624	<b>4.9833</b>	60.9779	59.2251	<b>2.8745</b>
	Box	39.2996	37.2232	<b>5.2837</b>	48.1626	45.4181	<b>5.6983</b>	44.3865	41.5619	<b>6.3637</b>
	ThrowCatch Average	84.0748	81.9438	<b>2.5346</b>	48.492	45.9944	<b>5.1504</b>	/	/	/
HoG (C1)	Walking	45.8417	43.7909	<b>5.7381</b>	41.6827	39.2721	<b>5.9947</b>	48.6996	46.2453	<b>5.2668</b>
	Jog	30.7786	29.7702	<b>3.2765</b>	20.2406	19.4853	<b>3.7317</b>	38.259	37.2519	<b>2.6324</b>
	Gestures	35.2833	34.3592	<b>2.6191</b>	27.5999	26.6086	<b>3.5918</b>	26.9919	26.0356	<b>3.5429</b>
	Box	5.3718	5.2444	<b>2.3714</b>	39.9867	38.8397	<b>2.8685</b>	43.4735	42.8049	<b>1.5378</b>
	ThrowCatch Average	26.9904	26.3226	<b>2.4743</b>	40.9108	39.764	<b>2.8032</b>	32.2198	31.3732	<b>2.6276</b>
HoG (C2)	Walking	70.661	69.4619	<b>1.6971</b>	41.2717	40.6461	<b>1.5159</b>	/	/	/
	Jog	33.817	33.0317	<b>2.4876</b>	34.0019	33.0687	<b>2.9022</b>	35.2236	34.3664	<b>2.5852</b>
	Gestures	25.6649	24.9178	<b>2.9112</b>	17.4669	16.883	<b>3.3428</b>	32.0536	31.4839	<b>1.7774</b>
	Box	36.1562	35.8948	<b>0.7229</b>	25.0174	24.4919	<b>2.1002</b>	22.5577	22.0753	<b>2.1384</b>
	ThrowCatch Average	8.2509	7.8924	<b>4.345</b>	41.0384	40.7589	<b>0.6812</b>	37.409	37.5382	<b>-0.3456</b>
HoG (C3)	Walking	25.952	25.4622	<b>1.8874</b>	33.5624	33.103	<b>1.3689</b>	35.4483	34.9741	<b>1.3379</b>
	Jog	69.2615	68.8563	<b>0.5849</b>	38.06	37.7767	<b>0.7443</b>	/	/	/
	Gestures	33.0571	32.6047	<b>2.0903</b>	31.029	30.6027	<b>1.6475</b>	31.8672	31.5179	<b>1.227</b>
	Box	26.4685	25.6706	<b>3.0143</b>	16.2316	15.5688	<b>4.0835</b>	33.3515	32.5203	<b>2.4922</b>
	ThrowCatch Average	34.4813	34.0262	<b>1.3199</b>	26.0008	25.2859	<b>2.7493</b>	22.5078	22.0039	<b>2.2388</b>
Total (% Gain)	Walking	9.5843	9.2134	<b>3.8701</b>	36.7243	36.3498	<b>1.0198</b>	35.8515	37.286	<b>-4.0013</b>
	Jog	25.9197	25.425	<b>1.9087</b>	29.6339	29.4589	<b>0.5906</b>	30.8706	30.269	<b>1.949</b>
	Gestures	67.1347	65.7422	<b>2.0743</b>	38.2297	38.0795	<b>0.3929</b>	/	/	/
	Box	32.7177	32.0155	<b>2.4375</b>	29.3641	28.9486	<b>1.7672</b>	30.6453	30.5198	<b>0.6696</b>
	ThrowCatch Average	HoG (C1+C2+C3) : <b>5.0796</b>			HoG (C1) : <b>2.5147</b>			HoG (C2) : <b>1.2928</b>		
								HoG (C3) : <b>1.4067</b>		

Table 7: Evaluation using HoG features on HumanEva-I. Positive % Gain for each subject is shown in **bold**, and in **red** otherwise. In the table, / shows that the values are not available (no training samples); Average gives the averaged % Gain for the different motions of the same subject; C1 means image feature are computed only from the first camera; C1+C2+C3 means image features from three cameras are combined in a single descriptor. Columns TGP and HOTGP indicate the mean absolute error while the % Gain column indicates the percentage reduction on error.

Features	Motions	Subject 1			Subject 2			Subject 3		
		HSIC	HOHSIC	% Gain	HSIC	HOHSIC	% Gain	HSIC	HOHSIC	% Gain
HoG (C1C2C3)	Walking	159.6824	159.406	0.1730	175.6263	175.6051	0.0120	200.1092	200.1722	<b>-0.0315</b>
	Jog	182.5472	182.6827	<b>-0.0742</b>	196.0942	196.2373	<b>-0.0729</b>	204.6334	204.7445	<b>-0.0542</b>
	Gestures	121.9071	120.8305	0.8831	128.1372	127.128	0.78759	161.8518	160.9014	0.5872
	Box	150.7509	150.3133	0.29026	190.5383	189.7172	0.4309	194.1369	193.4358	0.3611
	ThrowCatch	188.2296	188.4557	<b>-0.1201</b>	145.4743	144.7525	0.4961	/	/	/
	Average	160.6234	160.5714	0.0839	167.1740	167.0846	0.0808	190.1828	190.1161	0.0888
HoG (C1)	Walking	159.6824	159.4031	0.17489	175.6263	175.6204	0.0033	200.1092	200.1728	<b>-0.0318</b>
	Jog	182.5472	182.7127	<b>-0.0906</b>	196.0942	196.2703	<b>-0.0898</b>	204.6334	204.7865	<b>-0.0748</b>
	Gestures	121.9071	120.829	0.88431	128.1372	127.0738	0.82991	161.8518	160.9037	0.5857
	Box	150.7509	150.3093	0.29293	190.5383	189.7167	0.4312	194.1369	193.4387	0.3596
	ThrowCatch	188.2296	188.3374	<b>-0.0572</b>	145.4743	144.6998	0.53246	/	/	/
	Average	160.6234	160.5714	0.0839	167.1740	167.0846	0.0808	190.1828	190.1161	0.0888
HoG (C2)	Walking	159.6824	159.4017	0.17574	175.6263	175.6094	0.0096	200.1092	200.1662	<b>-0.0285</b>
	Jog	182.5472	182.6946	<b>-0.0807</b>	196.0942	196.2758	<b>-0.0926</b>	204.6334	204.8042	<b>-0.0834</b>
	Gestures	121.9071	120.8318	0.88202	128.1372	127.0976	0.81134	161.8518	160.8771	0.6022
	Box	150.7509	150.3304	0.27895	190.5383	189.7168	0.43115	194.1369	193.4401	0.3589
	ThrowCatch	188.2296	188.3753	<b>-0.0774</b>	145.4743	144.6909	0.53856	/	/	/
	Average	160.6234	160.3267	0.2357	167.1740	166.6781	0.3396	190.1828	189.8219	0.2123
HoG (C3)	Walking	159.6824	159.4267	0.16009	175.6263	175.6623	-0.0204	200.1092	200.2031	<b>-0.0469</b>
	Jog	182.5472	182.744	<b>-0.1078</b>	196.0942	196.2974	-0.10361	204.6334	204.8073	<b>-0.0849</b>
	Gestures	121.9071	120.8289	0.88443	128.1372	127.0813	0.82406	161.8518	160.9025	0.5865
	Box	150.7509	150.3118	0.29129	190.5383	189.716	0.43159	194.1369	193.4405	0.3587
	ThrowCatch	188.2296	188.3351	<b>-0.0560</b>	145.4743	144.7051	0.52877	/	/	/
	Average	160.6234	160.3293	0.2343	167.1741	166.6924	0.3321	190.1828	189.838	0.2033
Total (% Gain)		HoG (C1+C2+C3) : <b>0.2566</b>			HoG (C1) : <b>0.2589</b>			HoG (C2) : <b>0.2589</b>		
					HoG (C3) : <b>0.2625</b>					

Table 8: Evaluation using HoG features on HumanEva-I. Positive *% Gain* for each subject is shown in **bold**, and in **red** otherwise. In the table, / shows that the values are not available (no training samples); Average gives the averaged *% Gain* for the different motions of the same subject; C1 means image feature are computed only from the first camera; C1+C2+C3 means image features from three cameras are combined in a single descriptor. Columns HSIC and HOHSIC (Gegen.) indicate the mean absolute error while the *% Gain* column indicates the percentage reduction on error.

Features	Motions	Subject 1		Subject 2		Subject 3	
		HSIC	HOHSIC	% Gain	HSIC	HOHSIC	% Gain
HoG (C1C2C3)	Walking	159.6824	159.6333	0.03069	175.6263	175.6285	-0.0012
	Jog	182.5472	182.5801	<b>-0.0180</b>	196.0942	196.1282	<b>-0.0174</b>
	Gestures	121.9071	121.7042	0.1664	128.1372	127.9456	0.14957
	Box	150.7509	150.6684	0.0547	190.5383	190.3837	0.0811
	ThrowCatch	188.2296	188.2713	<b>-0.0221</b>	145.4743	145.3374	0.0941
	Average	160.6234	160.5714	0.0839	167.1740	167.0846	0.0808
HoG (C1)	Walking	159.6824	159.6326	0.0311	175.6263	175.6299	<b>-0.0020</b>
	Jog	121.9071	121.704	0.1665	128.1372	127.9364	0.15667
	Gestures	182.5472	182.5845	<b>-0.0204</b>	196.0942	196.1347	<b>-0.0206</b>
	Box	150.7509	150.6677	0.0551	190.5383	190.3838	0.08113
	ThrowCatch	188.2296	188.2513	<b>-0.0115</b>	145.4743	145.3287	0.1001
	Average	160.6234	160.5680	0.0843	167.1740	167.0827	0.1126
HoG (C2)	Walking	159.6824	159.6331	0.0308	175.6263	175.6278	<b>-0.0009</b>
	Jog	121.9071	121.7045	0.1661	128.1372	127.9402	0.15374
	Gestures	182.5472	182.581	<b>-0.0184</b>	196.0942	196.1343	<b>-0.0204</b>
	Box	150.7509	150.6713	0.0527	190.5383	190.3839	0.0810
	ThrowCatch	188.2296	188.2578	<b>-0.0149</b>	145.4743	145.3272	0.1011
	Average	160.6234	160.5695	0.0832	167.1740	167.0826	0.1120
HoG (C3)	Walking	159.6824	159.6374	0.0281	175.6263	175.6382	<b>-0.0067</b>
	Jog	121.9071	121.704	0.1666	128.1372	127.9402	0.15374
	Gestures	182.5472	182.5894	<b>-0.0231</b>	196.0942	196.1389	<b>-0.0227</b>
	Box	150.7509	150.6681	0.0548	190.5383	190.3837	0.08115
	ThrowCatch	188.2296	188.2506	<b>-0.0111</b>	145.4743	145.3293	0.0997
	Average	160.6234	160.5699	0.0430	167.1740	167.0860	0.0610
Total (% Gain)		HoG (C1+C2+C3) : <b>0.0471</b>		HoG (C1) : <b>0.0846</b>		HoG (C2) : <b>0.0952</b>	
				HoG (C3) : <b>0.0952</b>			

Table 9: Evaluation using HoG features on HumanEva-I. Positive % Gain for each subject is shown in **bold**, and in **red** otherwise. In the table, / shows that the values are not available (no training samples); Average gives the averaged % Gain for the different motions of the same subject; C1 means image feature are computed only from the first camera; C1+C2+C3 means image features from three cameras are combined in a single descriptor. Columns HSIC and HOHSIC indicate the mean absolute error while the % Gain column indicates the percentage reduction on error.

Features	Motions	Subject 1			Subject 2			Subject 3		
		TGP	HOTGP	% Gain	TGP	HOTGP	% Gain	TGP	HOTGP	% Gain
HoG (C1C2C3)	Walking	37.4366	9.5482	74.4951	21.7661	6.0762	72.084	44.4345	9.7506	78.0562
	Jog	8.6656	2.3434	72.957	60.314	11.9035	80.2642	48.5744	9.0458	81.3775
	Gestures	49.8854	10.5647	78.822	52.4706	10.9267	79.1756	35.704	9.1127	74.4771
	Box	38.3083	9.5265	75.1321	52.3877	11.4781	78.0901	48.8305	11.0568	77.3567
	ThrowCatch	63.9985	11.78	81.5933	59.1893	11.6716	80.2808	/	/	/
	Average	39.6588	8.7525	76.5999	49.2255	10.4112	77.9789	44.3858	9.7414	77.8168
HoG (C1)	Walking	36.9087	9.7608	73.5541	21.6479	9.931	54.125	44.895	10.94	75.6321
	Jog	9.4207	2.5032	73.4284	60.7753	11.8101	80.5676	51.9379	32.982	36.4973
	Gestures	49.1918	10.6199	78.4112	52.5459	10.9897	79.0856	35.9421	9.2451	74.2779
	Box	38.042	9.5071	75.0089	52.8592	11.6581	77.945	48.8239	13.3002	72.7589
	ThrowCatch	63.0999	11.7392	81.3959	58.7804	12.8523	78.1351	/	/	/
	Average	39.3326	8.82604	76.3597	49.3217	11.4482	73.9716	45.3997	16.6168	64.7915
HoG (C2)	Walking	37.8241	0.0109	99.9711	20.1582	0.0097	99.9518	42.5441	0.0115	99.9729
	Jog	8.8519	0.0068	99.9231	59.6685	0.0108	99.9817	51.9699	0.0114	99.978
	Gestures	48.517	0.0118	99.9756	53.1385	0.0100	99.9811	35.9633	0.0112	99.9687
	Box	36.7858	0.0098	99.9733	59.3451	0.0110	99.9813	49.0821	0.0108	99.9779
	ThrowCatch	64.2616	0.0141	99.9779	52.2494	0.0097	99.9813	/	/	/
	Average	39.2480	0.0107	99.9642	48.9119	0.0103	99.9754	44.8898	0.0112	99.9743
HoG (C3)	Walking	21.4906	0.0108	99.9497	12.4445	0.0095	99.9236	25.0639	0.0118	99.9528
	Jog	4.3108	0.0061	99.8604	34.9702	0.0103	99.9703	29.1524	0.0115	99.9604
	Gestures	28.7849	0.0119	99.9587	29.9167	0.0097	99.9674	19.6575	0.0112	99.9429
	Box	22.2626	0.0094	99.9578	30.5953	0.0101	99.967	28.0667	0.0099	99.9645
	ThrowCatch	35.3846	0.0142	99.9599	33.3681	0.0103	99.969	/	/	/
	Average	22.4467	0.0104	99.9373	28.2589	0.0100	99.9594	25.4851	0.0111	99.9551
Total (% Gain)		HoG (C1+C2+C3) : <b>99.9506</b>			HoG (C1) : <b>77.4652</b>			HoG (C2) : <b>71.7076</b>		
								HoG (C3): <b>99.9713</b>		

Table 10: Evaluation using HoG features on HumanEva-I. Positive % Gain for each subject is shown in **bold**, and in **red** otherwise. In the table, / shows that the values are not available (no training samples); Average gives the averaged % Gain for the different motions of the same subject; C1 means image feature are computed only from the first camera; C1+C2+C3 means image features from three cameras are combined in a single descriptor. Columns TGP and HOTGP (**Gegen**) (1,5) indicate the mean absolute error while the % Gain column indicates the percentage reduction on error.